APPLICATION OF AUTOCATHODE IN A SUPERCONDUCTING ELECTRON RF INJECTOR FOR THE INDUSTRY ACCELERATOR

V.N.Volkov, S.G.Konstantinov, A.M.Kudryavtsev, O.K.Myskin, V.M.Petrov, A.G.Tribendis
Budker Institute of Nuclear Physics, Russia
D.Janssen, FZ-Rossendorf, Germany

Abstract

Recently, publications on the development of cold field emission cathodes with current high density at rather low voltage applied are very broadly spread [1,2]. In the work presented here, the computer simulation has been performed for one of the versions of application of such cathodes in a superconducting RF cavity of the electron injector designed for the industrial accelerator.

1 INTRODUCTION

A superconducting linear electron industrial accelerator is designed for a mean electron current of 5 mA and energy of up 10 MeV at RF frequency of 1300 MHz. The injector part of the accelerator consists of a superconducting cavity with the copper stem inside and the choke filter. Under the action of RF field, the electron beam is injected from the field emission cathode (autocathode) fixed at the copper stem end and it is accelerated in the cavity up to energy of 33 keV. Then, through the hole of 1 cm in diameter the beam goes to the accelerator (linac). The linac consists of 6.5 cells of TESLA structure. The accelerator-operating mode is a π-mode. Numerical calculations have shown that in the accelerator with the optimized geometry, all the particles injected from the autocathode are accelerated without interaction with the accelerator walls.

2 ACCELERATOR

The geometry of a superconducting industrial accelerator is presented in Fig.1. All the accelerator cells are stamped of a thin niobium sheet and then welded with an electron beam. Fig.1 shows the field pattern of an electric RF accelerating fields (oscillations are of π-mode).

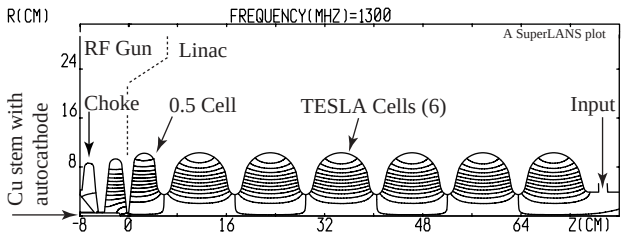

Fig.1. Geometry of the accelerator with RF field pattern.

The injector (RF-gun) is given on the left-hand side of the Figure 1. The geometry of a 6.5 cell linear accelerator (linac) is shown on the right-hand side of the Figure. An electron beam is injected to the linac from the injector through a 1-cm diameter hole in the niobium wall.

Fig.2 shows the schematic diagram of the accelerator control system. Frequency of generator is automatically tuned to the resonance frequency of the linac with the external Phase Locking Loop (PLL). Tuner-1 tunes the voltage in the injector to the work with beam current set automatically with the Feed Back loop (FB1). The additional feedback circuit (FB2) is designed for maintaining stable RF voltages at the linac cells.

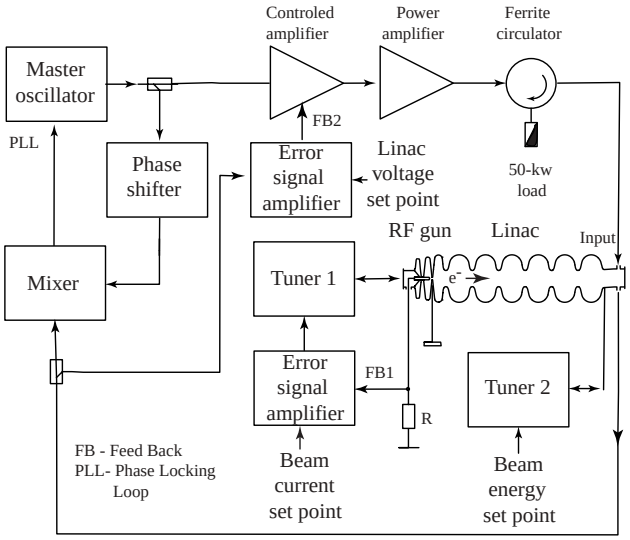

Fig.2 Schematic diagram of accelerator control circuits.

The shift to the other particle energy level in an electron beam is achieved by returning the linac by Tuner-2. In this case, in practice, the only cell «0.5 Cell» is returned since all the remaining TESLA cells of the linac are stronger. As a result, the redistribution of voltages occurs at the linac cells: one can either set the voltage increasing from the first to the last cell (see Fig.3) or the voltage dropping at the cells. In the first case, the particle energy will be higher and in the second case, the particle energy will be lower.

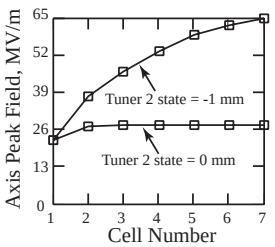

Fig.3. Peak RF electric fields in cells at the linac axis.

The beam power is varied by tuner-1. In this case, both RF voltage in the injector and RF field at the

Table 1. Accelerator parameters with both two extreme sets of Tuner-2.

Linac length returning by Tuner-2, mm	0			-1.0
Injector length returning by Tuner-1, mm	-0.03	-.006	0	-0.006
Linac generator power (beam power), kW	3.45	27	45	50
Resonance frequency, MHz	1300			1299.81
Beam particle energy, MeV	9.17			17
Power scattered at the linac walls, W	17.07			60.8
Maximum accelerating rate in the linac cells, MeV/m	15.9			33.4

autocathode are changed. At the same time the mean current and power of the beam are changed but the beam particle energy at the accelerator exit is remaining the same. Table 1 shows the accelerator parameters for two extreme sets of Tuner-2.

2 SHAPE OF AUTOCATHODE CURRENT PULSE

The dependence of the autocathode current density on the electric field intensity at the cathode is determined by the Fauler-Nordgeim formula:

$$J(E)=A\cdot E^2\cdot\exp(-B/E) \qquad (1)$$

where A and B coefficients are determined by the experimental curve of this dependence. J(E) is the autoemission current density in terms of A/cm^2, E is the intensity of RF electric field in terms of MV/m. We used the experimental dependence J(E) given in Ref.[1] and shown in Fig.4.

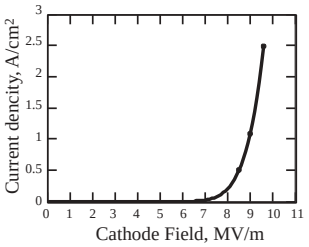

Fig.4. Autocathode current density as a function of the electric field intensity [1].

We obtained the following values of the coefficients:

$$A= 1042\ (MV/m)^{-2},\ B = 101.336\ MV/m$$

Dependence of the autocathode current density on the RF phase (φ) in the cavity is similar to the Gaussian formula. Represent it as a product of the Gauss formula by the correcting coefficient K(φ):

$$J(\varphi)=K(\varphi)\cdot J_{max}\cdot\exp(-0.5\cdot\varphi^2/\sigma^2) \qquad (2)$$

Here J_{max} (J_{max} = 2.5 A/cm^2) is the current density at the moment of maximum intensity at the cathode E_{max} (E_{max} = 9.6 MV/m). σ is a rms length of the current pulse (σ= 15.5°). Functions J (φ) and K (φ) are presented in Figures 5 and 6, respectively.

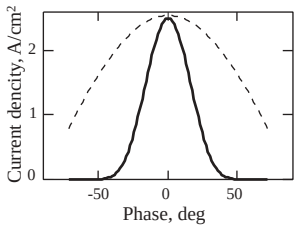

Fig.5 Autocathode current density as a function of RF phase. Upper curve is the intensity of RF field at autocathode.

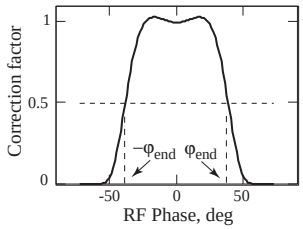

Fig. 6 Correcting factor K as a function of RF phase φ.

One can assume (see Fig.6) that for phase angles $-\varphi_{end}<\varphi<\varphi_{end}$ K (φ) ~1. For all other phase angles, K(φ) tends to 0. In calculations we used the cathode current shape in the form of the Gaussian curve cut at $\varphi=\pm\varphi_{end}$, when $K(\varphi_{end}) = 1/2$.

3 INJECTOR

The injector and autocathode geometric are given in Figure 7. The autocathode consists of a nanocrystallic carbon layer [1] applied at the spherical surface of the refractory metal tablet. The tablet of 1.54 mm in diameter is tightly inserted into a hole at the copper stem end.

The copper stem of 1 cm in diameter with the autocathode at its end is placed inside the superconducting cavity. Maximum RF power scattered in the stem is 31 W. The stem is cooled with liquid nitrogen applied inside the stem from outside along pipes having no contact with liquid helium. The stem has electric contact with the cavity body through the resistor only (R, see fig.2). The voltage on the resistor is proportional to a beam current. It is used in Feed Back 1 (FB1).

The choke filter protects the stem-fixing device against RF power from the cavity. Tests of the stem fixing device and choke filter have shown good positive result [3].

The cavity body (Fig.7) is stamped and welded of a thin niobium sheet. The body is rigid enough to withstand the external atmospheric pressure. The cone walls have an inclination of 6 degrees thus enabling the qualitative etching and washing the inner surface of the cavity (without the cathode stem) by pumping the solvents of acids and washing water through the cavity.

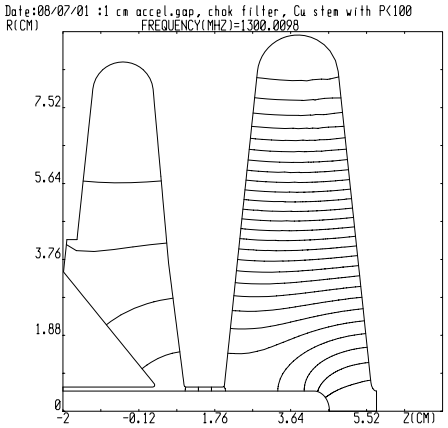

Fig.7. A superconducting niobium cavity of a 1300 MHz injector with field pattern of electric RF.

Table 2. Cavity parameters.

QUALITY FACTOR (T=2K).... 1.6285+005
STORED ENERGY ..... 1.9244-003 J
TRANSIT TIME FACTOR ... .9970E+00
EFFECTIVE IMPEDANCE .... 5.049+001 OHM
SHUNT IMPEDANCE ..... 8.22241 MOHM
MAXIMUM MAG. FIELD ..... 5.539+003 A/M
MAXIMUM ELEC.FIELD ..... 9.600+000 MV/M
P_{Nb}= 0.0043 W, T=2K
P_{Cu}=30.992 W, T=77K
Coupling factor of injector-linac is $2.4 \cdot 10^{-4}$.
Phase shifting of injector RF voltage is less then 0.25°.
Resonant frequency is less then 1300 MHz by 1.6 MHz.

4 LINAC

The geometry of a 6.5 cell linear accelerator (linac) is shown on the right-hand side of the Figure 1. Linac cavity parameters calculated with the use of the SuperLANS program [4] is shown in the table 3.

Table 3. Linac cavity RF parameters with Tuner-2 state=0

Cavity radius, cm	10.33
Cavity length, cm	84.7152
Quality factor (T=2K)	8.59e+009
Stored energy, J	19.808
Maximum mag. field, A/m	5.118+004
Maximum elec. field, MV/m	33.28

5 DYNAMICS

Table5 shows the bunch parameters calculated with use of the PARMELLA program [5]. The first column represents parameters of the bunch outgoing from the accelerating structure (z=86 cm). The second column shows parameters of the bunch passing through the 90-bending magnet at a distance of 250 cm from the cathode. In order to reduce the bunch radius we used the focusing solenoid. The solenoid is place at a distance of 50 cm from the structure edge and its comprises 43.4 windings.

Table 4. Bunch parameters in the operation sets Tuner-1 = 0 mm and Tuner-2 = 0 mm.

Cathode peak field, MV/m	9.6	
Injection bunch length (rms), degree	15.5	
Total injection bunch length, degree	87	
Cathode radius, cm	0.077	
Distance from cathode; cm	86.1	250.1
Average Energy, MeV	9.16	9.16
Energy spread (rms), %	5.54	5.48
Transv. norm. emitt.(rms), cm·mrad	6.06	21.84
Long. emitt.(rms), KeV.cm	190.8	181.6
Rms bunch radius, cm	1.08	0.166
Rms bunch length, cm	0.488	0.469

Energy spread in an electron beam is given in Fig.8. At the tail part of bunches, there are particles with a low energy of down to 1.66 MeV and low current. These particles are cut in the bending magnet. The power released by the cut particles in the collector depends on the maximum particle energy in the cut part of the bunch. This dependence is shown in Fig.9. Power released by the cut part of the bunch does not exceed 47 W

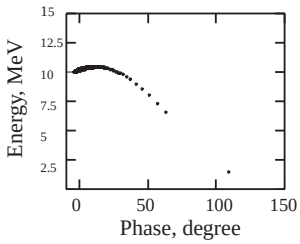

Fig.8 Energy spread of particles in a bunch.

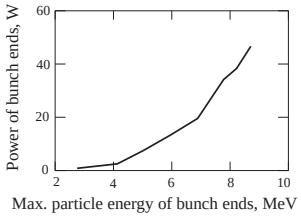

Fig.9 Particle power at the tail part of the bunch cut in the bending magnet.

5 REFERENCES

[1] A.T. Rakhimov. *Field-emission cathodes (cold emitters) on nanocrystal-carbon and nano-diamond films: physics, technology, application*, Physics-Uspekhi 43 (9), September 2000.
[2] A.N.Obraztsov, et al.. *Diamond and Ralated Mater.* 6 (1997) 1124.
[3] *On the way to a superconducting RF-gun: first measurement with the gun cavity*,
E.Barhels, H.Buttig, F.Gabriel, E.Grosse, D.Janssen, A.Bushuev, M.Karliner, S.Konstantinov, S.Kruchkov, O.Myshkin, V.Petrov, I.Sedlyarov, A.Tribendis, V.Volkov, W.Sandner, I.Will, P.v.Stein, H.Vogel, A.Matheisen, M.Pekeler, Ch.Haberstroh, A.Thiel, Nuclear Instruments and Methods in Physics Research, A 445 (2000) 408-412.
[4] D.G. Myakishev, V.P. Yakovlev, PAC99, New York, 1999, pp. 2775-2776.
[5] L. Young, *PARMELA*, LA-UR-96-1835, LANL (1996)